FAI/82-17

REVISION 1 - 7/16/82

DRAFT

Fauske & Associates, Inc.

16W070 West 83rd Street

Burr Ridge, Illinois 60521

(312) 323-8750

ANALYSIS OF NOMINAL HEAT REMOVAL CAPACITY OF THE CRBRP IN THE NATURAL CIRCULATION MODE

June, 1982

TABLE OF CONTENTS

		Page
1.0	INTRODUCTION	1
2.0	SODIUM RE-ENTRY AND DRY-OUT CRITERIA UNDER DECAY HEAT POWER CONDITIONS	3
2.1	Simple Re-Entry Criterion for Sub-Assembly Geometry	4
3.0	NATURAL CIRCULATION HEAT REMOVAL ANALYSIS	7
4.0	NATURAL DRAFT CAPACITY FOR THE PROTECTED AIR COOLED CONDENSERS (PACCs)	19
4.1	General Configuration	19
4.2	Pressure Difference For Natural Draft	26
4.3	System Flow Capacity	26
4.4	Air Side Heat Transfer Coefficient	26
4.5	Overall Heat Transfer Coefficient	30
4.6	Energy Removal from the PACCs	32
4.7	Heat Removal Rates by Ultimate Heat Sinks	34
5.0	SUMMARY	41
6.0	REFERENCES	43

LIST OF TABLES

Table No.		Page
2.1	Comparison of Heat Fluxes from Empirical Correlation [Eq. (2.4] and the Simple Re-Entry Criterion [Ineq. (2.2)]	6
4.1	PACC Air Flow Rate Vs Pressure Drop	28

LIST OF FIGURES

Figure No.		Page
3.1	Hydraulic Head for Natural Circulation	8
3.2	Hydraulic Pressure Drop Equation for the CRBRP Primary System	10
3.3	Comparison of Best Estimate and DEMO Results at 1000s	11
3.4	Hot and Cold Leg Temperature-Time Histories for One Loop Natural Circulation	12
3.5	Hot and Cold Leg Temperature-Time Histories for Two Loop Natural Circulation	13
3.6	Hot and Cold Leg Temperature-Time Histories for Three Loop Natural Circulation	14
3.7	Decay Power and Heat Removal Rates vs. Time for One Loop Natural Circulation	15
3.8	Decay Power and Heat Removal Rates vs. Time for Two Loop Natural Circulation	16
3.9	Decay Power and Heat Removal Rates vs. Time for Three Loop Natural Circulation	17
4.1	Protected Air Cooled Condenser	20
4.2	Protected Air Cooled Condenser	21
4.3	Fin Tube Coils	22
4.4	PACC Closed Loop Schematic (Shown During Normal Plant Operation - PACC Hot Standby)	23
4.5	The Piping and Instrumentation Diagram for the PACC Portion of the Steam Generator Auxiliary Heat Removal System	24
4.6	Dimensions and Calculated Surface Area of the Finned Tube	25
4.7	Schematic of PACCs for Natural Draft Operation	27
4.8	PACCs Flow Rate vs. Pressure Drop	29

LIST OF FIGURES (Continued)

Figure No. Page

4.9 Average Friction and Heat Transfer Data for Flow Over Five Different Arrangements of 3/8 in. Diameter Tube Bundles in the Laminar and Transition Regime 31

4.10 Steam and Air Temperature Variation in the PACCs 33

4.11 Heat Removal Rate by Venting vs. Time for One Loop Natural Circulation 35

4.12 Heat Removal Rate by Venting vs. Time for Two Loop Natural Circulation 36

4.13 Heat Removal Rate by Venting vs. Time for Three Loop Natural Circulation 37

4.14 Cumulative Mass of Steam Vented During a One Loop Natural Circulation Event 38

4.15 Cumulative Mass of Steam Vented During a Two Loop Natural Circulation Event 39

4.16 Cumulative Mass of Steam Vented During a Three Loop Natural Circulation Event 40

1.0 INTRODUCTION

As part of the probabilistic risk assessment (PRA) of the CRBRP, a variety of loss of heat sink (LOHS) accidents are being examined as events which might lead to core damage. Current evaluations of whether an event will lead to core damage have been based on design criteria which allow for little structural damage to a component and also include the normal design conservatisms to account for uncertainties in material properties, operating conditions and loads, etc. Because of these conservatisms many branches of the LOHS event trees have been designated as leading to core damage, although some heat sinks of limited capacity are available during the accident sequence. Two examples are a one-loop natural circulation event with a forced draft PACC and SGAHRS vent as heat sinks and a one-loop natural circulation event with a natural draft PACC and SGAHRS vent as heat sinks. The PRAs are based on best estimates and permit in some instances more extensive damage before failure than do design analyses. Three areas of conservatism which may have a significant, unfavorable impact on the PRA have been identified and are discussed in this report. The replacement of the conservative evaluations with "best estimate" ones may result in eliminating a significant fraction ($\sim$ 50%) of the core damage states currently being predicted.

The three areas of conservatism discussed in the following three sections of the report have a direct effect on the natural circulation heat removal capacity of the CRBRP systems. The areas deal with (1) localized boiling in the core under decay power with flow coastdown, (2) natural circulation heat removal under "quasi-steady state" conditions and (3) PACC heat removal capacity under natural air draft conditions. Accepting boiling in the core on a "best estimate" basis results in a large extension of the time

before core damage would occur and permits one to ignore the short term (< 1/2 hour) effects in the core during a natural circulation event. Then in the longer term (> 1/2 hour) the heat removal from the primary system by natural circulation can be estimated by assuming that quasi-steady conditions exist through the heat transport systems. Finally a heat sink credit is taken for the heat removal capacity of the PACCs under natural draft conditions by using "best estimate" analysis. Combining the results from three areas gives the best estimate of the CRBRP response to the loss of all AC power, i.e., natural circulation with turbine-driven feedwater and a natural draft PACC unit. The results of the analyses in the three areas of conservatism are presented in the next three sections; in the last section a summary of the current work is presented and further work is discussed which will extend the best estimates of the CRBRP heat removal capacity during natural circulation events.

2.0 SODIUM RE-ENTRY AND DRY-OUT CRITERIA UNDER DECAY HEAT POWER CONDITIONS

In the natural circulation analysis for CRBRP one criterion used for design purposes is that the sodium temperature must remain below boiling point, i.e., 938°C. For a best estimate analysis local boiling in the core is permitted because it does not prevent, in itself, the reactor to be brought eventually to a cooled-down condition. This section provides the technical basis for permitting local boiling and establishes sodium re-entry and dry-out criteria.

Based upon previous studies [1] of the accident progression for a hypothetical loss-of-heat-sink with scram in an LMFBR, incipient sodium boiling is expected to occur as the primary system sodium temperature approaches the saturation temperature. At this time (3 to 4 hours into the accident) the decay heat has fallen to approximately 1% of full power.* At this power level the critical assumption is made that sustained dryout is taken to coincide with incipient boiling [1,2] i.e., no sodium re-entry is allowed after boiling initiation with the result that fuel meltdown is predicted to occur with sodium still present in the upper plenum.

However, in this report we will illustrate through the use of first principle analysis of hydrodynamic requirements related to the sodium re-entry phenomenon which clearly suggests that the above assumption is overly conservative and that in fact the core must be uncovered of sodium before sustained dryout and fuel overheating are possible. On this basis, fuel disruption, if

*If not natural circulation is assumed following pump coastdown, incipient boiling would initiate at about 3 to 4% decay power.

it can occur at all*, will not take place before about 100 hours into the postulated accident as compared to earlier estimates of 3 to 4 hours. The simple re-entry criterion developed specifically for the subassembly geometry is also compared with a low flow convection, high quality critical heat flux criterion based upon experimental data including liquid metals. Heat flux values predicted by these two criteria are shown to be in excellent agreement.

2.1 Simple Re-Entry Criterion for Subassembly Geometry

In considering the potential for sodium re-entry the effects of the rod bundle geometry and associated two-dimensional phenomena must be taken into account [4]. Since the subassembly wall is not a heat sink and the flow to power ratio is considerably higher in the wall subchannels than in the central subchannels, the liquid flow next to the hexcan wall has no limitation in terms of the critical heat flux phenomenon, i.e., the wall channels can be running full of liquid while the central subchannels are experiencing dryout. In order to sustain dryout within the pin bundle portion of the subassembly, the vapor velocity and corresponding frictional pressure drop gradient must at least equal or exceed the gravitational pressure drop gradient corresponding to liquid sodium in the unheated hexcan wall channels so as to avoid refilling or re-entry of coolant. For the interconnected channel system typified by the subassembly geometry this physical requirement can be simply stated as follows:

$$u_g \geq \sqrt{\frac{2\rho_\ell D_h g}{f_g \rho_g}} \tag{2.1}$$

*The effect of natural insulation heat losses at elevated temperatures may prevent such an event altogether [3].

where ρ_ℓ and ρ_g are the density of liquid and vapor respectively, D_h is the hydraulic diameter, f_g is the vapor friction factor and g is the gravitational constant. The heat flux that corresponds to Ineq. (2.1) is given by

$$q \geq \sqrt{\frac{2\rho_\ell \rho_g g D_h}{f_g}} (A/\pi D \ell_h N)(\Delta h_i + h_{fg}) \qquad (2.2)$$

where A is the flow cross-sectional area of the subassembly, D is the fuel pin diameter, ℓ_h is the heated length, N is the number of fuel pins in the assembly, Δh_i is the liquid subcooling enthalpy and h_{fg} is the latent heat of vaporization. Thus for prototypic core conditions such as CRBRP one obtains a value for the minimum required heat flux to prevent re-entry at zero subcooling of approximately 8.4 w/cm^2. This heat flux corresponds approximately to 6% of the average nominal operating power. Only a modest increase of approximately 20% is seen by accounting for maximum subcooling (Δh_i = 582 J/g), i.e., q ≈ 10 w/cm^2.

A potential re-entry limitation provided by the single-channel geometry portion of the subassembly, i.e., downstream of the fuel pin section, also need to be examined. For the channel dimension involved, the flooding condition can be determined by the well known Kutateladze criterion [5].

$$u_g \geq K \rho_g^{-1/2} [(\sigma g(\rho_\ell - \rho_g)]^{1/4} \qquad (2.3)$$

Where K is the Kutateladze stability parameter, and σ is the liquid surface tension. Using a value of K of 3.0 which corresponds to flooding of liquid films or transition from slug to annular flow, one obtains u_g = 2400 cm/s. The corresponding velocity in the fuel pin section is (2400)(101.4/43.4) = 56-7 cm/s. Since this velocity is slightly larger than the value given by Ineq. (2.1), we conclude that Ineq. (2.2) provides a reasonable estimate of the fuel pin heat flux that must be exceeded in order to prevent refilling or re-entry of liquid sodium.

The equivalent critical heat flux value provided by Ineq. (2.2) is compared below to the following modification of the original Katto [6] correlation* by considering a typical LMFBR subassembly geometry [7].

$$q_c = 0.25\, Gh_{fg} \left(\frac{\sigma\rho_\ell}{G^2 \ell_h}\right)^{0.043} \frac{D_h}{\ell_h} \left[1 + \frac{P_w}{\zeta_h} \left(\frac{G^2 \ell_h}{\sigma\rho_f}\right)^{0.043} \frac{\Delta h_i}{h_{fg}}\right] \tag{2.4}$$

where G is the mass flow rate. The above correlation is compared to values predicted by Ineq. (2.2) in Table 2.1; the agreement is excellent.

Table 2.1

COMPARISON OF HEAT FLUXES FROM EMPIRICAL CORRELATION [EQ. (2.4)] AND THE SIMPLE RE-ENTRY CRITERION [INEQ. (2.2)]

T_i	CHF Eq. (2.4)	Re-Entry Ineq. (2.2)
420°C	$\sim$ 10 w/cm^2	$\sim$ 10 w/cm^2
800°C	$\sim$ 8.5 w/cm^2	$\sim$ 8.7 w/cm^2
No Subcooling	$\sim$ 8 w/cm^2	$\sim$ 8.4 w/cm^2

*Katto's original correlation was based upon critical heat flux data (liquid metals) relevant to the low flow convection (natural circulation) high quality nearly saturated inlet conditions regime of interest.

3.0 NATURAL CIRCULATION HEAT REMOVAL ANALYSIS

Natural circulation analysis of the CRBRP shows that the system performance (e.g., temperature histories, heat removal rates) is strongly influenced in the short term by several factors which causes some temperatures and flows to change markedly within the first half-hour. Detailed calculations, by the DEMO code for example, are needed to predict the system variables with accuracy. The large heat capacity of the primary system would limit in the early stage of the event the average temperature increase to ~ 55 °C/hr ~~40°C/hr~~ for the conservative case of an adiabatic primary system. This fact and the acceptability of local boiling in the core means that the evaluation of core damage during a natural circulation event can focus on the longer term effects. In this section the assumptions used in long term heat removal analysis of natural circulation are explained and the results are presented and discussed for circulation in one, two, and three loops. The scope of this analysis is to determine the heat removal rate from the primary system to the steam generator system; the ultimate heat sink for the cases without any feedwater is analyzed in the following section.

The best estimate natural circulation calculations were based on basic principles and CRBRP performance characteristics known from detailed DEMO analyses [8]. The hydraulic head equation given in Fig. 3.1 describes the system adequately for the quasi-static conditions which exist after ~ 1/2 hour of natural circulation. In this time regime the cold leg temperature, T_c, has reached equilibrium with the saturation temperature in the steam drum because the IHX and evaporator are very efficient at low flow rates. Decay power changes relatively slowly and inbalances between Q_{in} and Q_{out} are dampened by the large heat capacity of the primary system hot leg. Thus the

HYDRAULIC HEAD

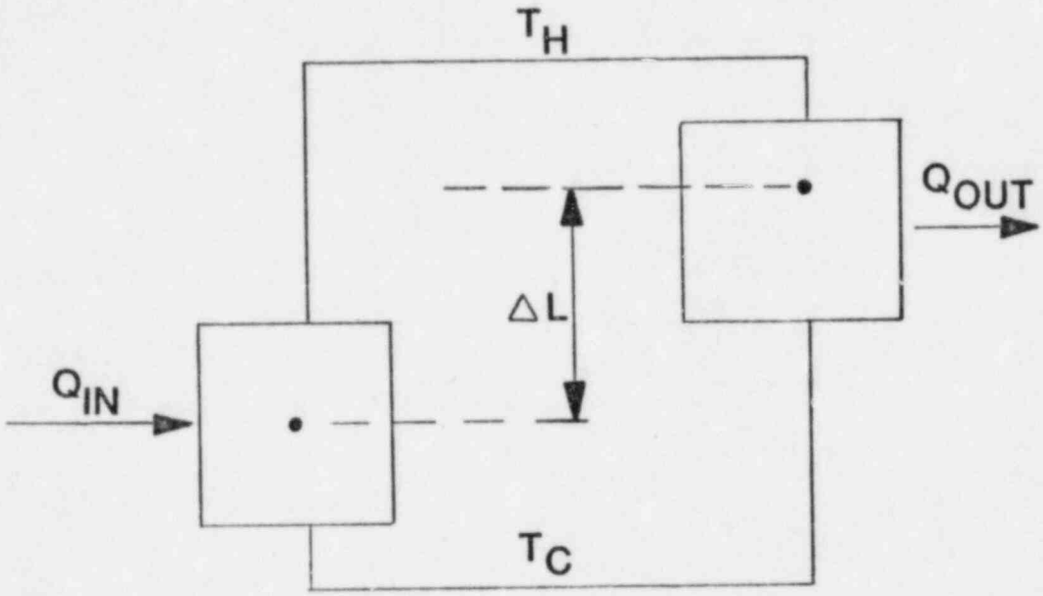

$$\Delta P_H = \rho g \beta \Delta T \Delta L$$

where $\Delta T = T_H - T_C$

Fig. 3.1 Hydraulic Head for Natural Circulation.

hot leg can also be characterized by a single value of T_H at any given time after natural circulation has been in effect for over ~ 1/2 hour. The hot leg temperature is obtained by an iterative process of allocating the decay heat input between natural circulation heat removal and heat capacity storage.

The hydraulic head is balanced by the frictional pressure drop, which is a function of the flow rate through the sections of CRBRP primary system. The pressure drop equation is given in Fig. 3.2. Plots of the frictional coefficients (K_i) vs. normalized flow rates in the most recent CRBRP natural circulation study [8] were used in the best estimate calculations. The flow rate is calculated from the hydraulic balance equation, and then the heat removal rate is obtained from the product of the flow rate, sodium heat capacity and temperature drop along the IHX. The best estimate values of the flow rate and system temperatures compare quite favorably with DEMO results at a 1000 seconds into natural circulation, as shown in Fig. 3.3.

The heat removal rate for natural circulation was calculated for one, two, and three loop operation using the model described above. The decay power values used in the CRBRP design calculations were reduced by 17% to obtain best estimate values. The final cold leg temperatures were taken as 315°C, which is the steam drum saturation temperature at SGAHRS operating conditions. The hot and cold leg primary system temperatures are given in Figs. 3.4, 3.5, and 3.6 for one, two, and three loop operation. In all three cases the hot leg temperatures peak early in the transient a few degrees above the full power temperature and then steadily drop as the primary system cools down. The cold leg temperature is programmed to approach 315°C early in the transient. The plots of the decay power and the heat removal rates by natural circulation in one, two, and three loops in Figs. 3.7, 3.8, and 3.9, respectively, show that natural circulation heat removal overtakes decay power

HYDRAULIC PRESSURE DROP

$$\Delta P_f = K_1 W_1^2 + K_2 W_2^2 + K_3 W_3^2 + K_4 W_4^2$$

where ΔP_f = frictional pressure drop

K_i = flow-dependant constant for section i

W_i = flow velocity through section i

i = 1 core

i = 2 pump with locked rotor

i = 3 check valve

i = 4 piping, IHX, etc.

Fig. 3.2 Hydraulic Pressure Drop Equation for the CRBRP Primary System.

	APPROX. METHOD	DEMO
T_H(°C)	511	493
T_C(°C)	268	257
ΔT(°C)	243	236
W/W_o(%)	2.9	$\sim$ 3.1

Fig. 3.3 Comparison of Best Estimate and DEMO Results at 1000s.

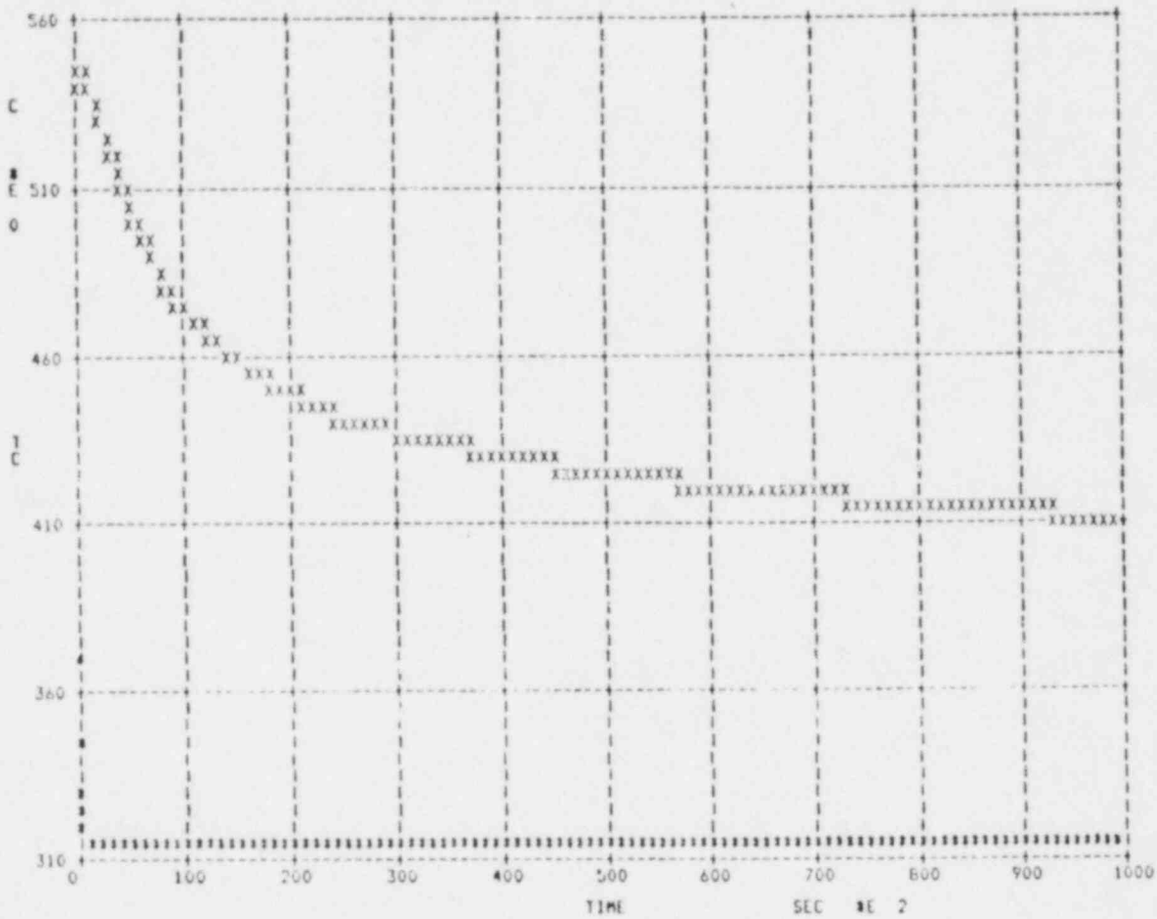

Fig. 3.4 Hot and Cold Leg Temperature-Time Histories for One Loop Natural Circulation.

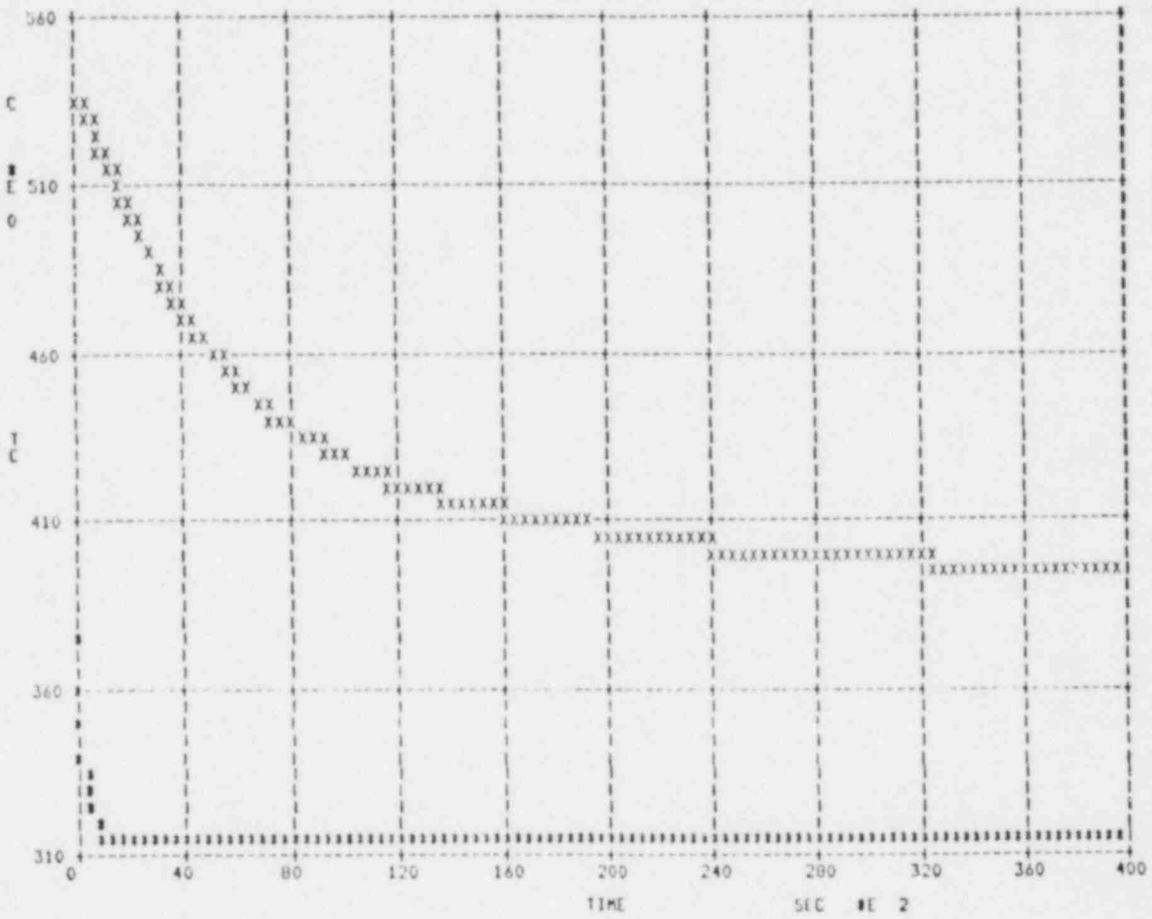

Fig. 3.5 Hot and Cold Leg Temperature-Time Histories for Two Loop Natural Circulation.

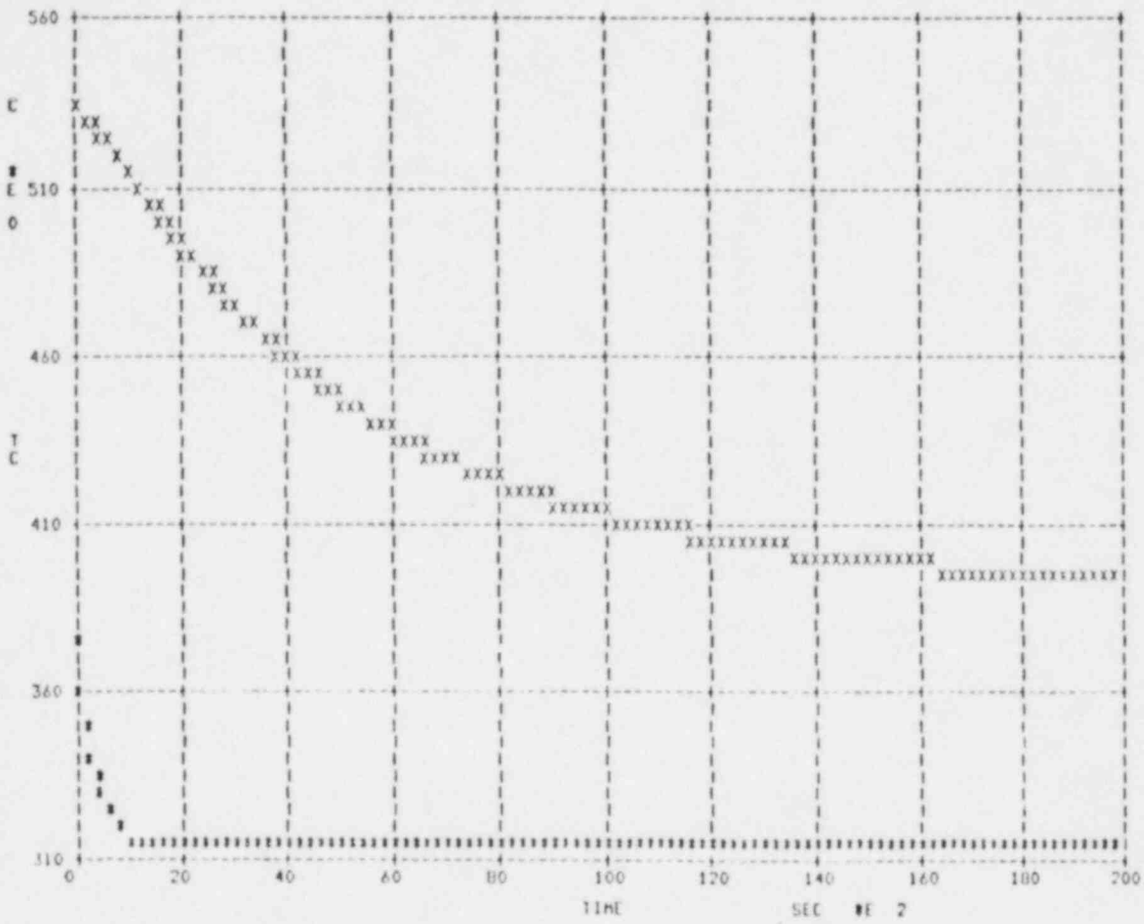

Fig. 3.6 Hot and Cold Leg Temperature-Time Histories for Three Loop Natural Circulation.

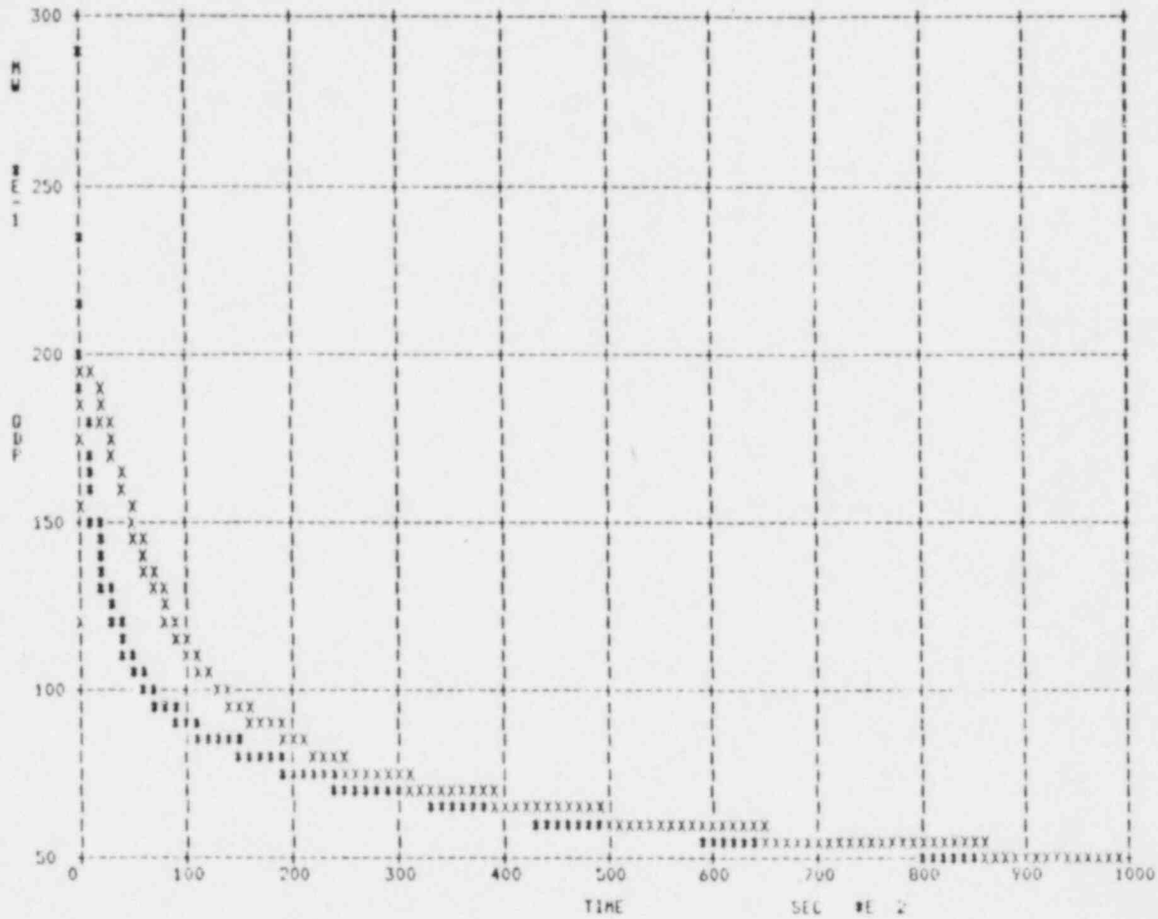

Fig. 3.7 Decay Power and Heat Removal Rates vs. Time for One Loop Natural Circulation.

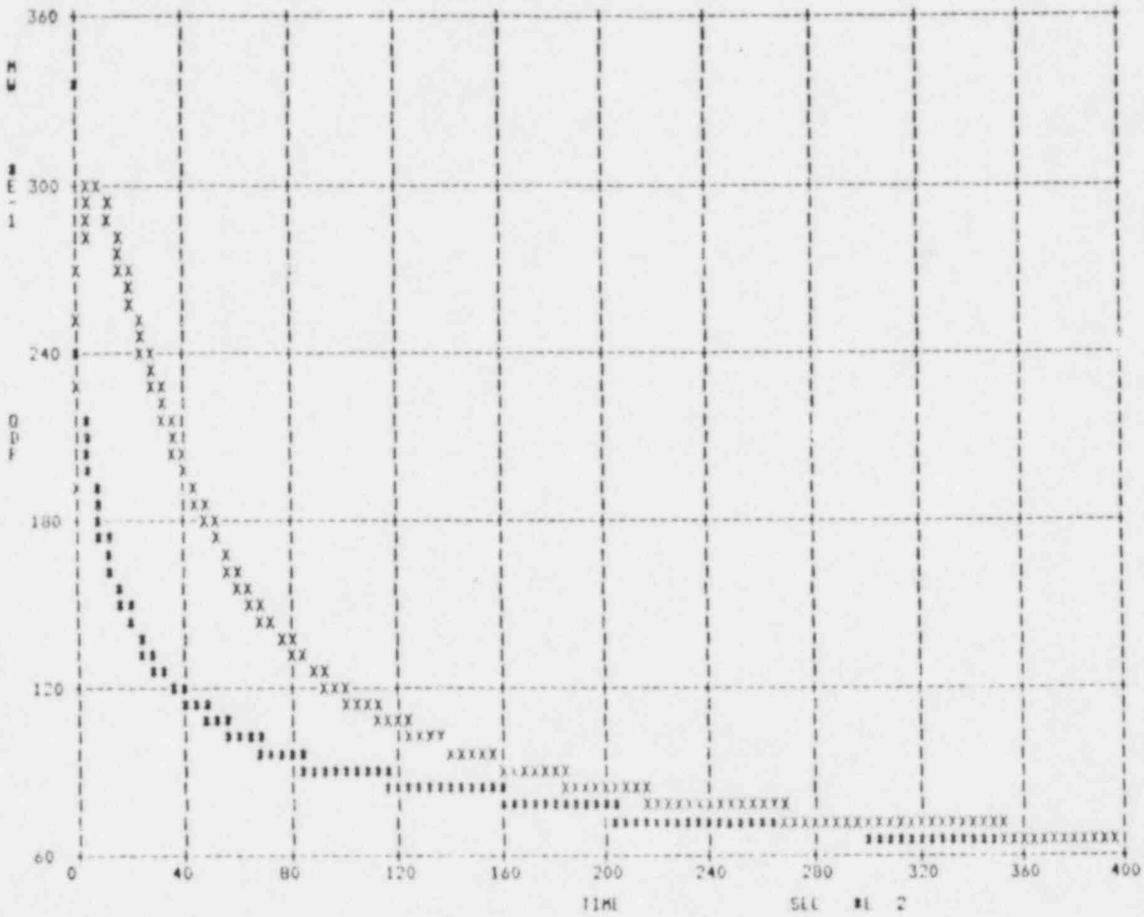

Fig. 3.8 Decay Power and Heat Removal Rates vs. Time for Two Loop Natural Circulation.

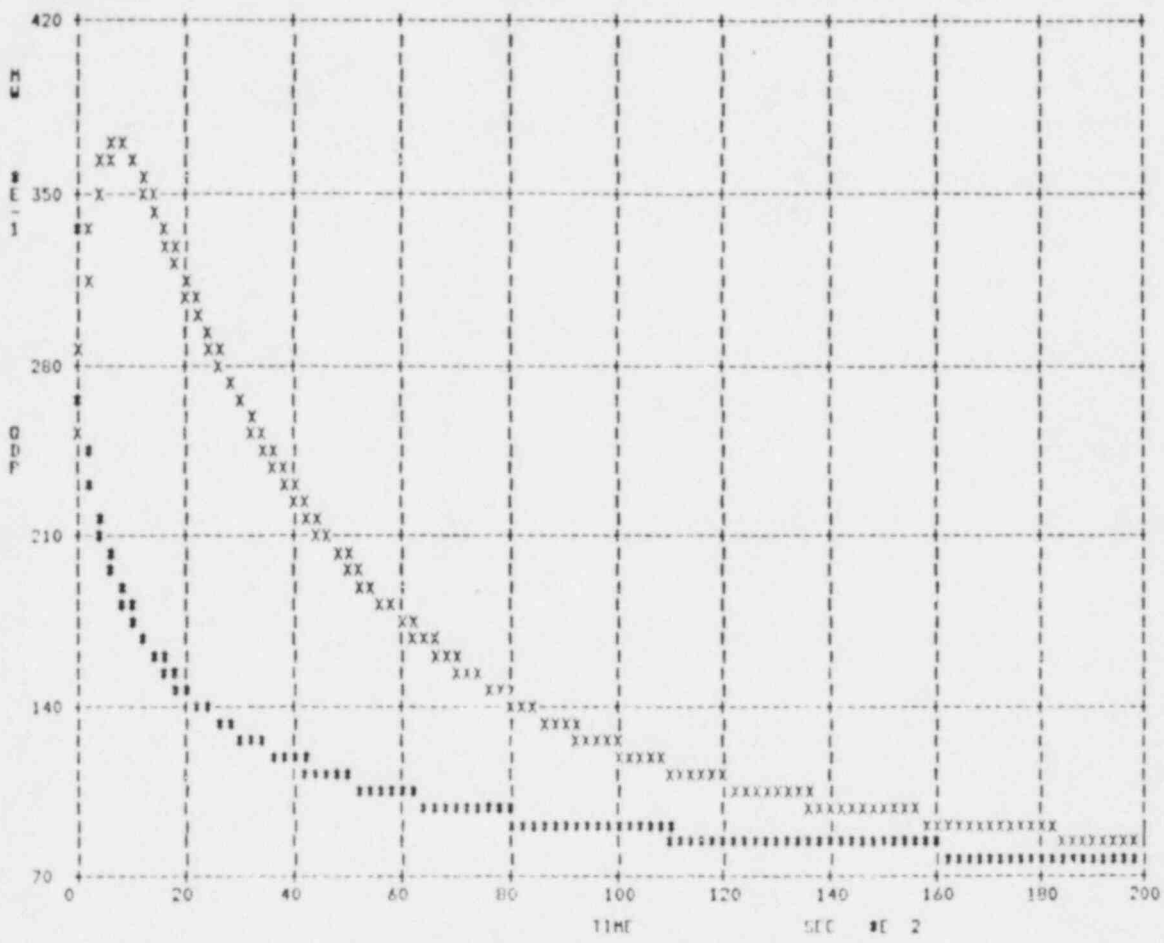

Fig. 3.9 Decay Power and Heat Removal Rates vs. Time for Three Loop Natural Circulation.

production in about 1000 seconds, even with only one loop. In less than a half-hour the natural circulation heat removal rates peaks and then steadily decreases as the ΔT driving force also diminishes. The results show that the CRBRP has very good natural circulation capabilities and that primary system temperatures correspond to those experienced in a mild transient, as long as a heat sink exists.

4.0 NATURAL DRAFT CAPACITY FOR THE PROTECTED AIR COOLED CONDENSERS (PACCs)

In assessing the response of the CRBRP system to a transient such as a total loss of AC power or an inability to supply auxiliary feedwater to the steam generators, the PACCs would play an essential role in both establishing the ultimate heat sink and the response time of the steam side. Since these units are part of the heat transfer circuit during normal operation, they would be available for immediate heat removal in such a postulated sequence. At the beginning of the sequence the inlet and outlet louvers to these units are assumed to open. The resulting natural draft flow and the corresponding heat removal capacity is evaluated below.

4.1 General Configuration

The PACCs units are illustrated in Fig. 4.1 with the flow paths being given in Fig. 4.2. Each unit consists of 50 finned tubes arranged in a spiral as illustrated in Fig. 4.3. These tubes are connected to an inlet and outlet header and are supplied steam from the top of the steam drum with the condensate draining back to the recirc pump header as illustrated in Figs. 4.4 and 4.5. The major resistances to heat removal are through the wall of these tubes and the convective heat removal off the outer surfaces of the tubes and the fins. Both the tubes and fins are constructed of carbon steel with the details of the fins being illustrated in Fig. 4.6. With this configuration, the air flow passes through the bank of spiral tubes and into the central region of the coil with the exhaust flow traveling through the outlet louvers and up through the exhaust stack. For these evaluations the exhaust stack is assumed to be 10 m high.

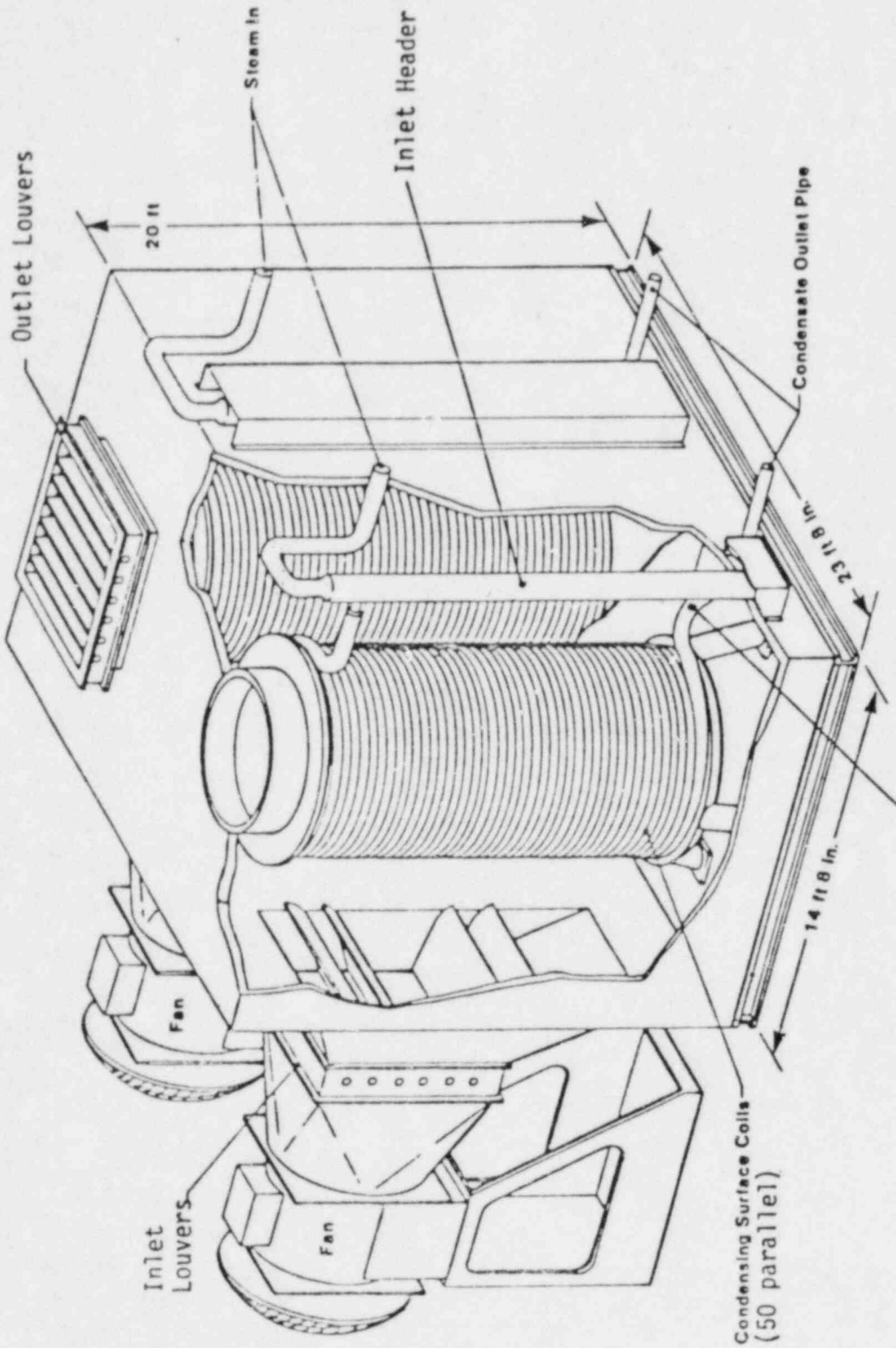

Fig. 4.1 Protected Air Cooled Condenser.

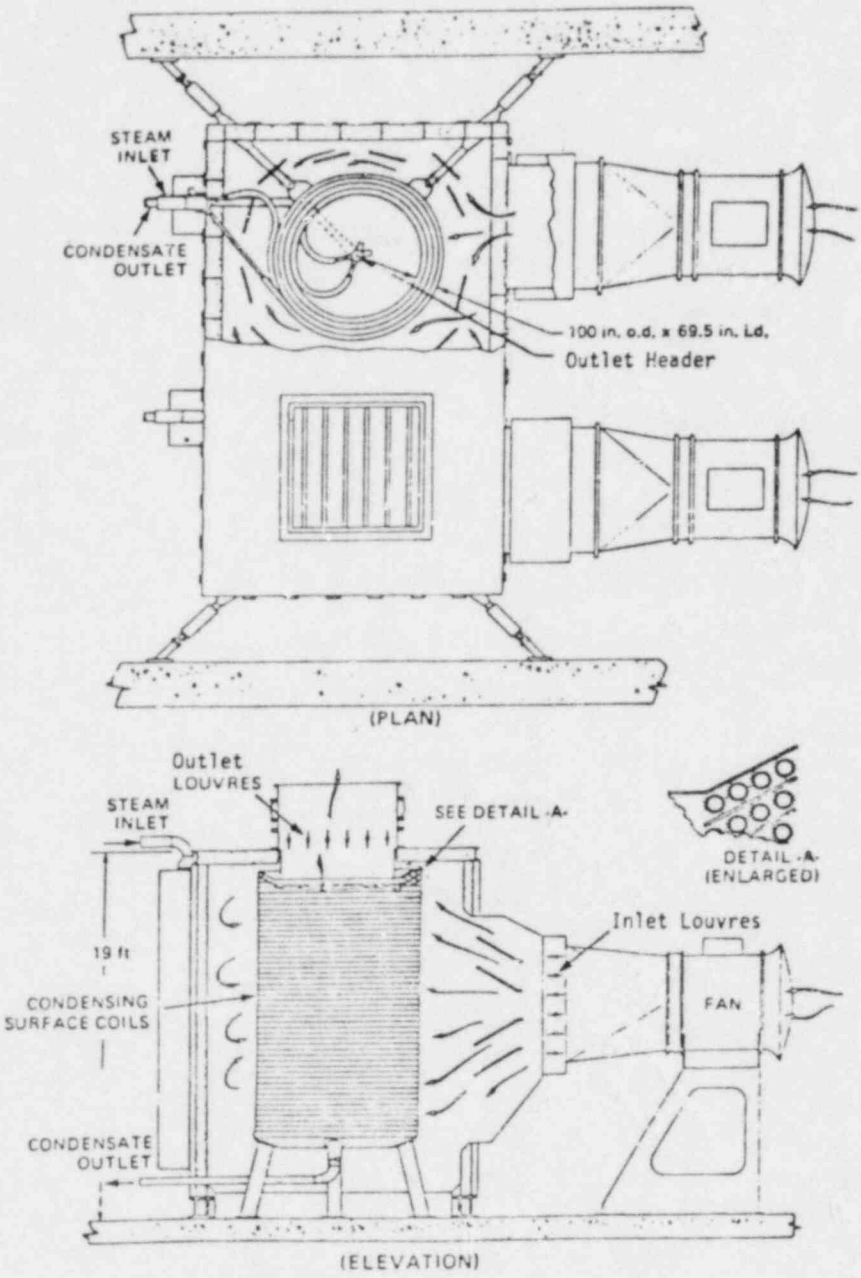

Fig. 4.2 Protected Air Cooled Condenser.

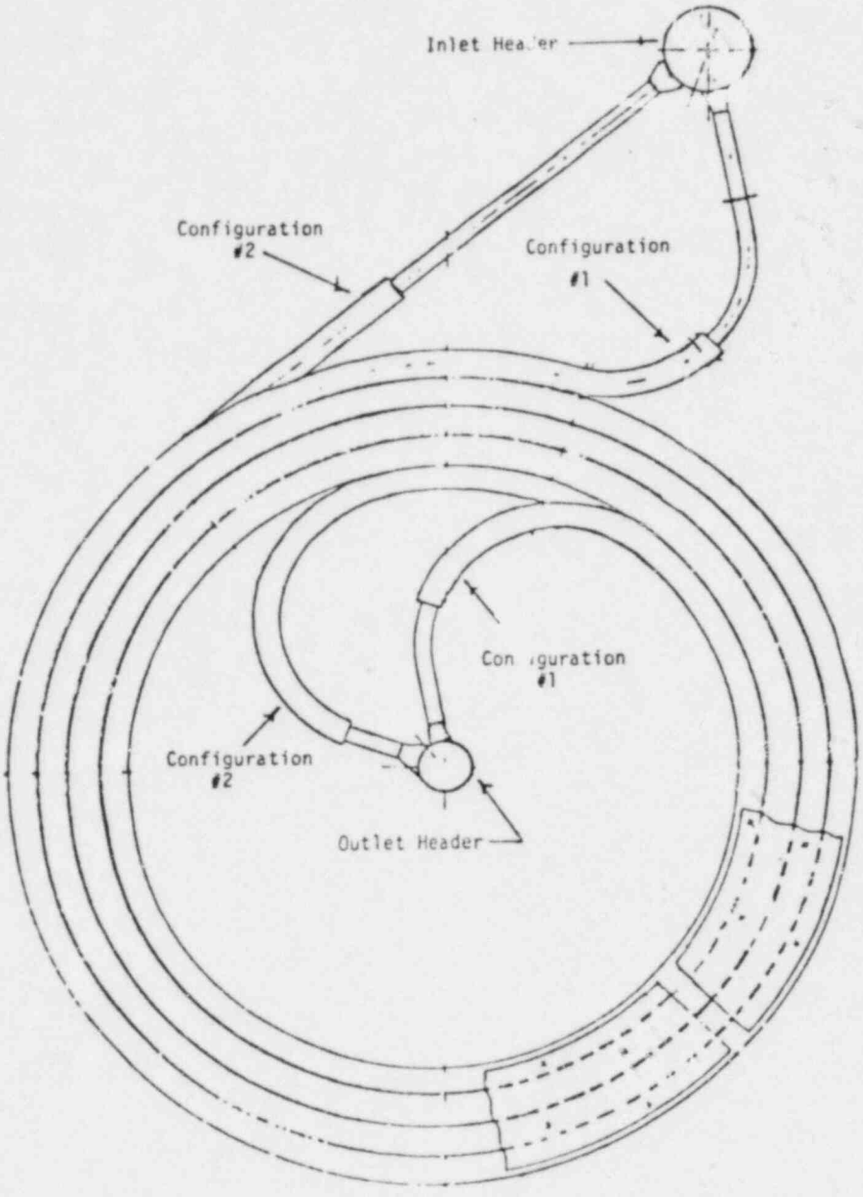

Fig. 4.3 Fin Tube Coils.

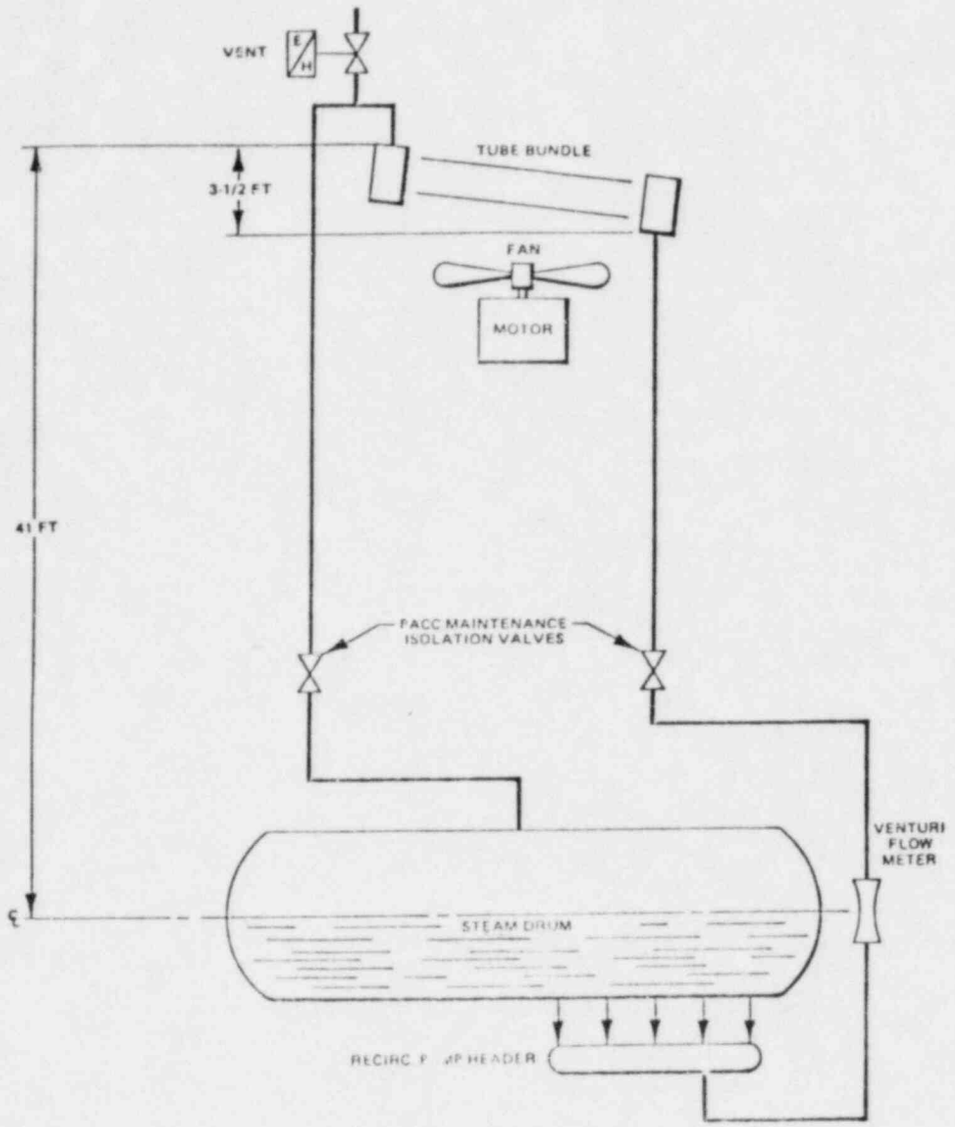

Fig. 4.4 PACC Closed Loop Schematic (Shown During Normal Plant Operation - PACC Hot Standby).

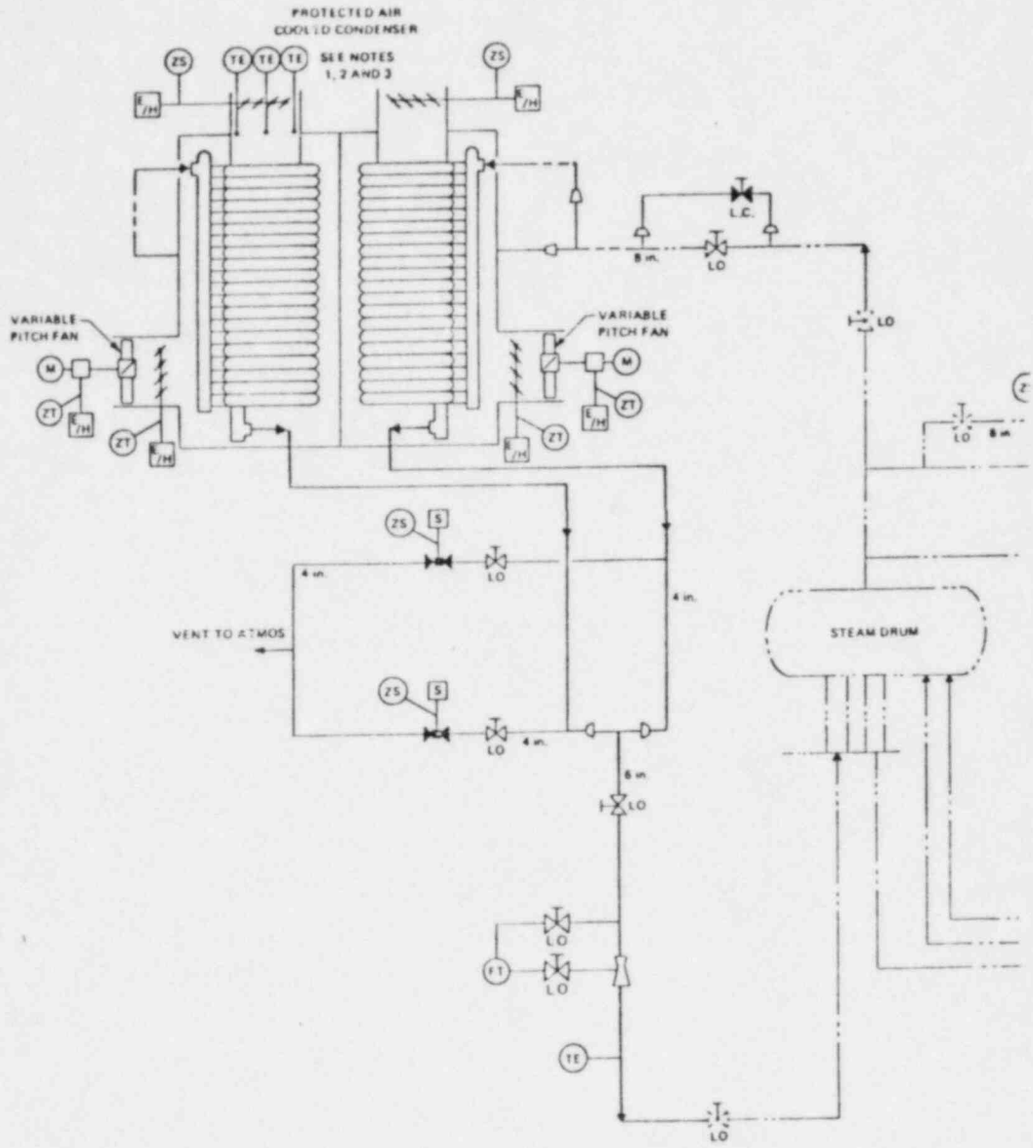

Fig. 4.5 The Piping and Instrumentation Diagram for the PACC Portion of the Steam Generator Auxiliary Heat Removal System.

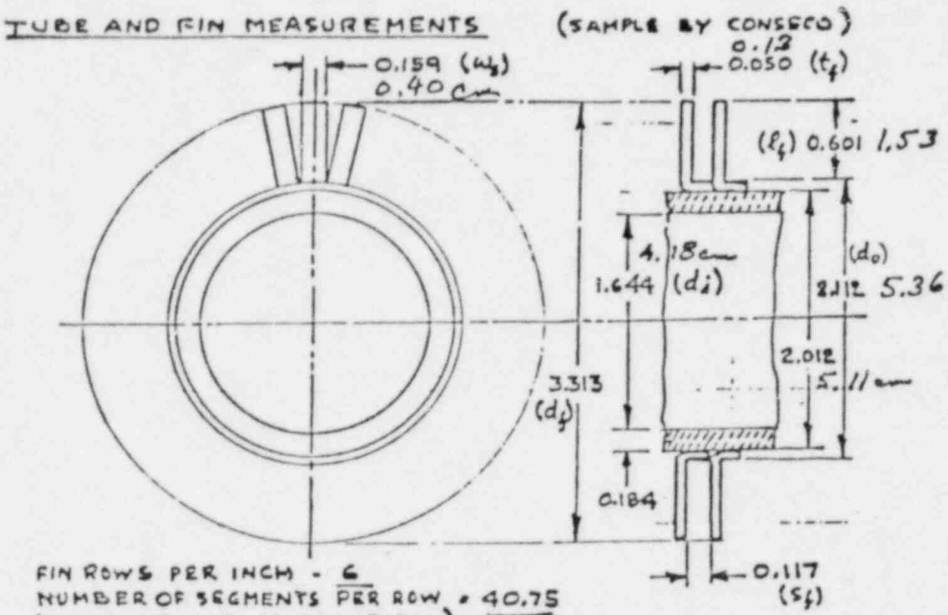

CALCULATED FIN-SIDE SURFACE

O.D. FIN HEEL (2.112")	0.3882	SQ. FT. PER FT.
FIN FACES	3.8990	" " "
FIN EDGES	1.3865*	" " "
TOTAL SURFACE	5.6387*	" " "

Fig. 4.6 Dimensions and Calculated Surface Area of the Finned Tube.

4.2 Pressure Difference For Natural Draft

Considering the schematic illustration for the PACCs shown in Fig. 4.7, the driving pressure for natural draft through the units can be expressed by

$$\Delta P = (\rho_{ao} - \rho_{ai})gh \tag{4.1}$$

and considering the air to be a perfect gas this can be expressed in terms of the inlet and outlet temperatures as

$$\Delta P = \frac{P}{R}\left(\frac{1}{T_{ao}} - \frac{1}{T_{ai}}\right)gh \tag{4.2}$$

A typical air inlet temperature would be 300°K (80°F) with the outlet temperatures under these conditions ranging from 500°K to 550°K (440°F - 530°F). For these two ranges, the pressure difference available for air flow is between 45.6 and 51.8 Pa.

4.3 System Flow Capacity

Evaluations of the forced convection flow through the PACCs unit have been made and are reported in Ref. [9]. Considering all the resistances in the system, the resulting values are tabulated in Table 4.1 in both English and SI units. In addition, these are graphically represented in Fig. 4.8 and compared with an expression relating the pressure drop and the square of the flow rate.

$$\Delta P = 0.43\ W^2 \tag{4.3}$$

For an average driving pressure of 48 MPa, the air flow rate would be 10.6 kg/sec.

4.4 Air Side Heat Transfer Coefficient

As discussed in Ref. [10], the heat transfer coefficient over tube bundles can be represented as a function of the dimensionless grouping

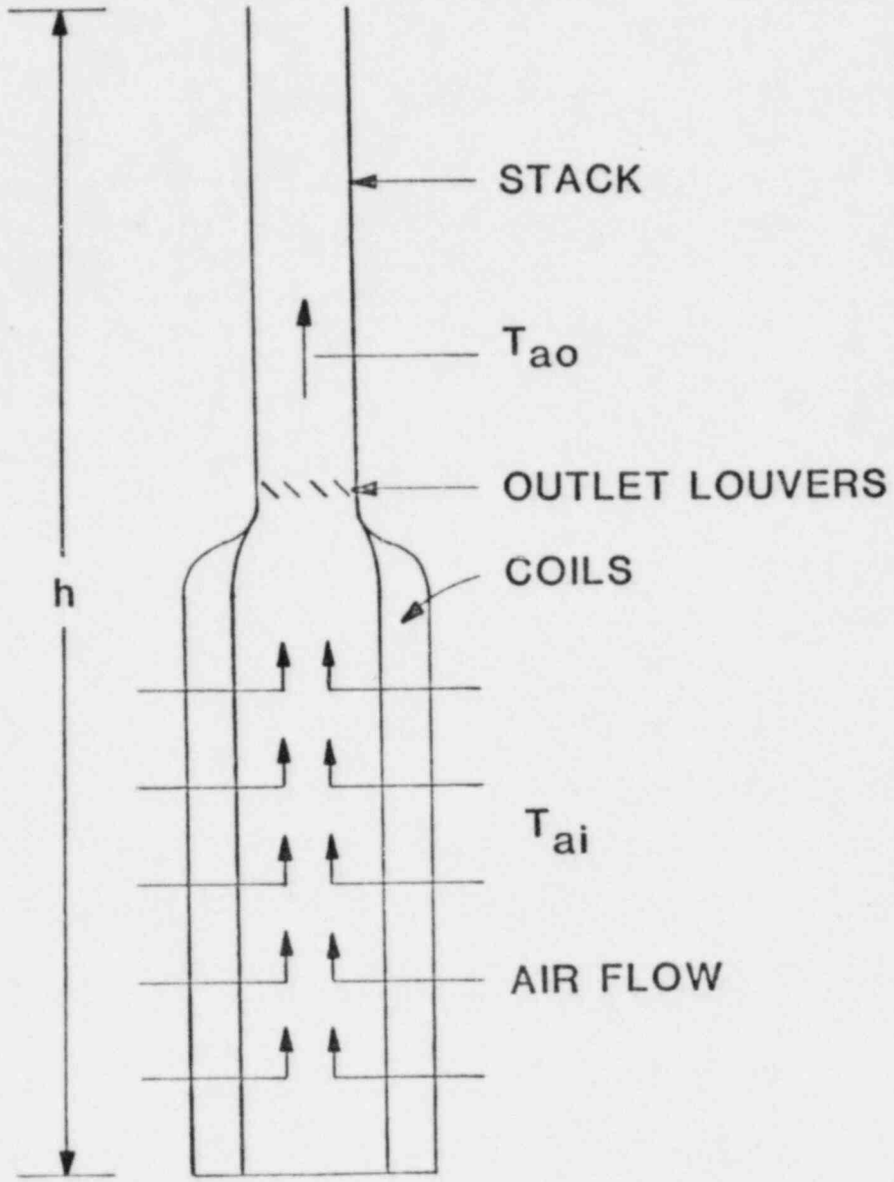

Fig. 4.7 Schematic of PACCs for Natural Draft Operation.

Table 4.1

PACC AIR FLOW RATE VS PRESSURE DROP

Mass Flow		Pressure Drop	
lbm/hr	kg/sec	Inches of Water	Pa
124,259	15.7	0.4281	106.5
165,679	20.9	0.7810	194.4
207,099	26.1	1.1939	297.2
248,519	31.4	1.7025	423.8
289,939	36.6	2.3077	574.4
331,358	41.8	2.9713	739.6
372,778	47.1	3.7085	923.1

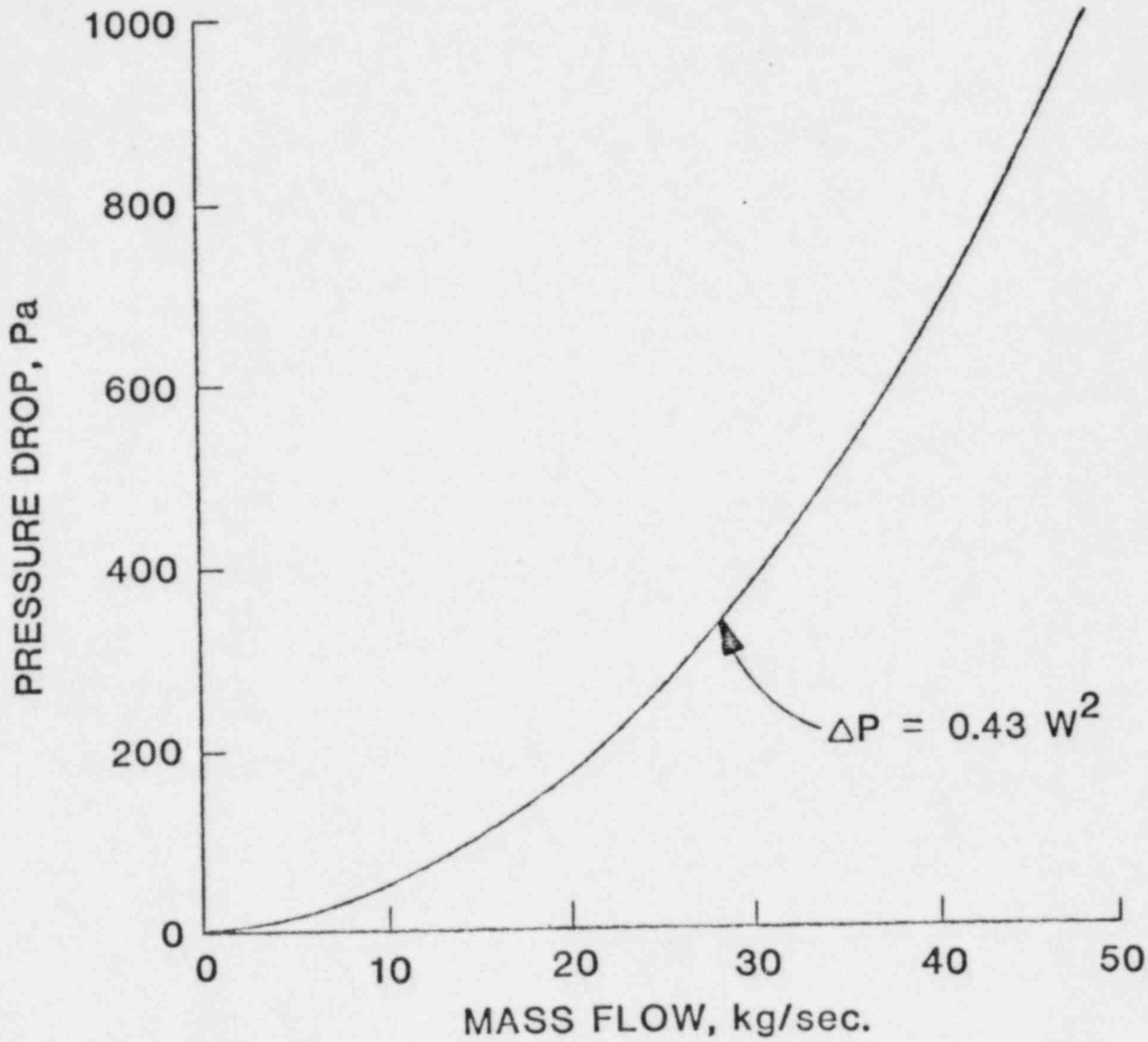

Fig. 4.8 PACCs Flow Rate vs. Pressure Drop.

$$j = \frac{h_a}{C_p G_{max}} Pr^{2/3} \left(\frac{\mu_a}{\mu_b}\right)^{0.14} = \phi\left(\frac{G_{max} D_o}{\mu_a}\right) \tag{4.4}$$

where the term G_{max} is the maximum flux density between the minimum tube spacing. Ignoring the presence of fins and the viscosity variation and assuming that the air flows uniformly radially inward toward the center of the cooling unit, the maximum flux density is ~ 0.41 kg/m^2-sec. The above dimensionless number is then ~ 1000 and the corresponding value for j, as shown in Fig. 4.9, is ~ 0.025. Evaluating the gas side heat transfer coefficient yields a value of 0.013 kw/m^2-°K, or in English units 2.4 btu/hr-ft^2/°F. This value is well within the range of those values considered for natural draft behavior.

4.5 Overall Heat Transfer Coefficient

For this analysis the thermal resistance on the steam side is neglected and the principle thermal resistances are conduction through the tubes and convective heat removal off the tube and the fins by the air. Since these are series resistances the overall heat transfer effectiveness can be expressed by

$$UA = \frac{1}{\frac{\ln(r_o/r_i)}{2\pi k_t L} + \frac{1}{hA}} \tag{4.5}$$

where r_0 is the outer radius of the tube and the fin base (2.68 cm) and r_i is the inner diameter of these tubes (2.09 cm). For the values given above, the product of UA would be 13 kw/°C.

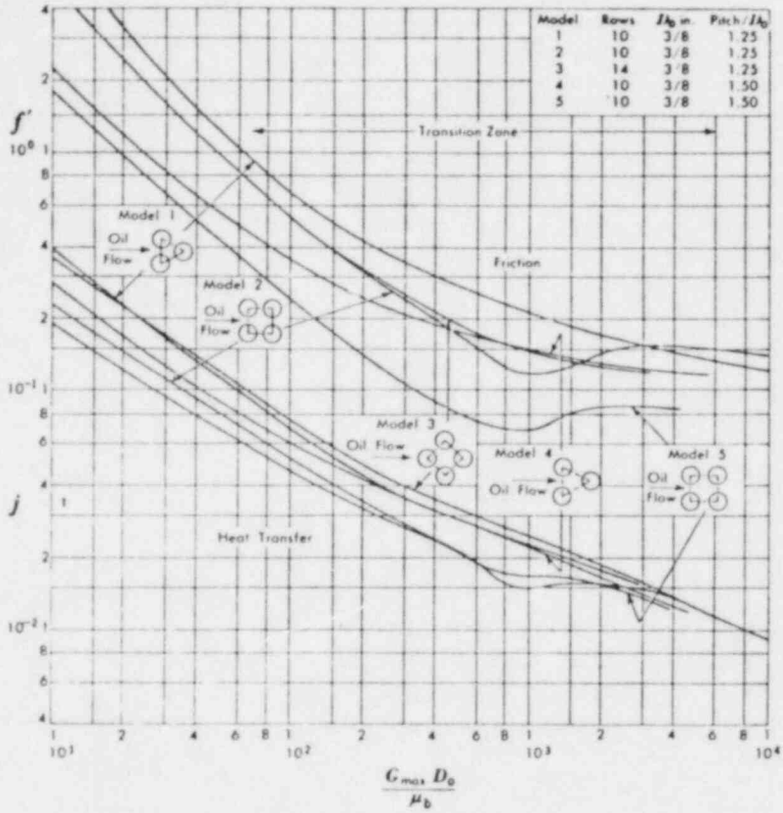

Fig. 4.9 Average Friction and Heat Transfer Data for Flow Over Five Different Arrangements of 3/8 in. Diameter Tube Bundles in the Laminar and Transition Regime.

4.6 Energy Removal from the PACCs

As an air cooled condenser, the temperature variation for the steam side and air side within the PACCs can be represented as shown in Fig. 4.10. The heat transfer rate can be expressed as

$$\dot{Q} = UA\ \overline{\Delta T} = Wc_P\ (T_{ao} - T_{ai}) \tag{4.6}$$

where

$$\overline{\Delta T} = \frac{\Delta T_a - \Delta T_b}{\ln \frac{\Delta T_a}{\Delta T_b}} \tag{4.7}$$

since the steam side temperature remains constant, this expression can be rearranged to

$$\ln \frac{\Delta T_a}{\Delta T_b} = \frac{UA(T_{ao} - T_{ai})}{Wc_P(T_{ao} - T_{ai})} = \frac{UA}{Wc_P} \tag{4.8}$$

or

$$\frac{T_s - T_{ai}}{T_s - T_{ao}} = e^{\frac{UA}{Wc_P}} \tag{4.9}$$

Solving this expression for the outlet air temperature (T_{ai}) results in the following expression.

$$T_{ao} = T_s - (T_s - T_{ai})e^{-\frac{UA}{Wc_P}} \tag{4.10}$$

As illustrated in a previous section, the gas flow rate varies as the square root of the pressure drop and the pressure difference developed by the natural draft is relatively insensitive to the outlet air temperature. As an average value sufficient for these evaluations, we will consider the pressure difference to be 48 MPa which provides for a gas flow rate of 10.6 kg/sec.

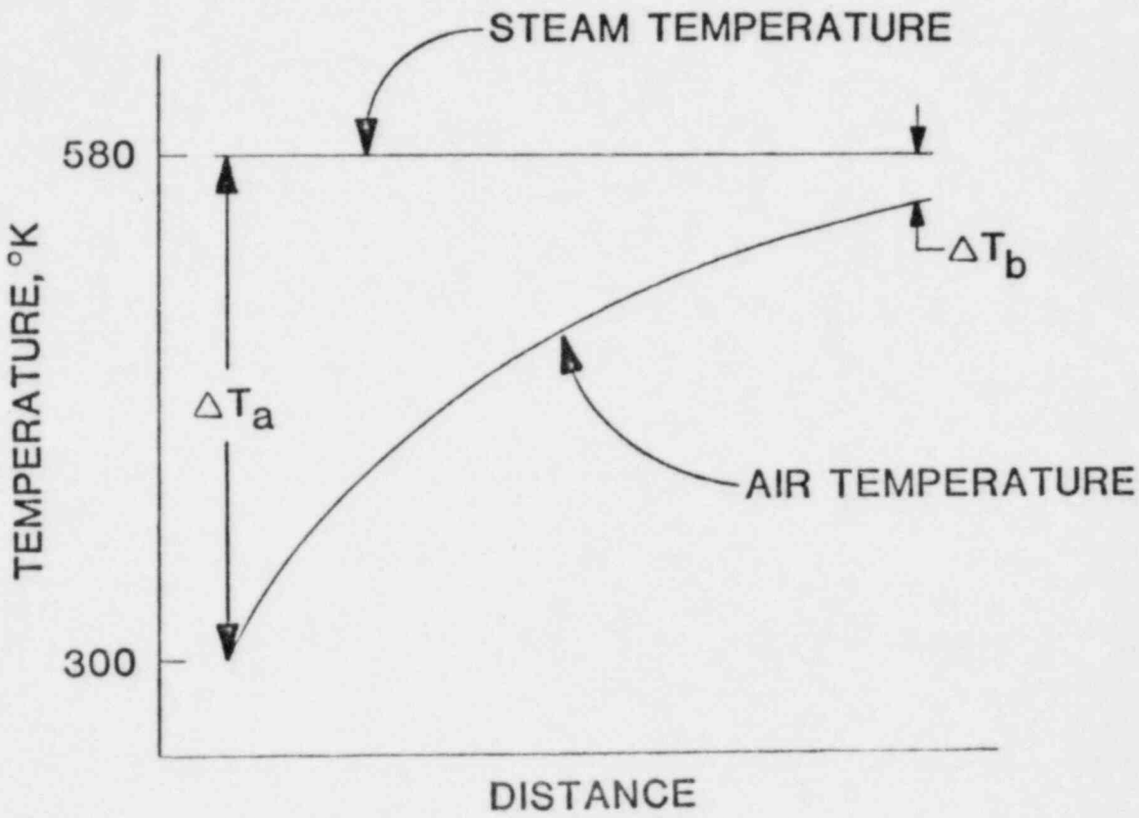

Fig. 4.10 Steam and Air Temperature Variation in the PACCs.

4.7 Heat Removal Rates by Ultimate Heat Sinks

The heat which is removed from the primary system by natural circulation is assumed to be transferred through the IHX and evaporator in a very efficient manner. The amount of heat removed from the primary system is assumed to equal the amount of heat used to generate the steam which flows to the steam drum. The heat is removed from the steam drum by condensing steam in the PACCs and by venting the excess steam to the atmosphere. The amount of the heat removed by venting at a given time is obtained by subtracting the constant PACC heat removal rate of 4.24 Mw/loop from the current natural circulation heat removal rate. The venting rates in Mw are plotted for one, two, and three loop natural circulation cases in Figs. 4.11, 4.12, and 4.13. The venting rate is converted into the mass of the steam which is integrated to give the cumulative mass of steam vented from the system. These results are given in Figs. 4.14, 4.15, and 4.16.

The heat removal rate by venting peaks within a half hour and then decreases steadily until it reaches zero. The three cases show significant differences in the time to the end of venting, about 9600 seconds (2 2/3 hrs) for three loop operation and over 100,000 sec ($\sim$ 27 hours) for one loop operation. The total mass of the steam vented also differs significantly, between 50,000 kg and 177,000 kg for three and one loop operation, respectively. Note that the total water inventory in the drums, pipes and evaporators is $\sim$ 50,000 kg and in the protected water storage tank is $\sim$ 250,000 kg. The analysis shows that most of the steam is vented as a result of cooling down the primary system rather than as a result of removing decay power.

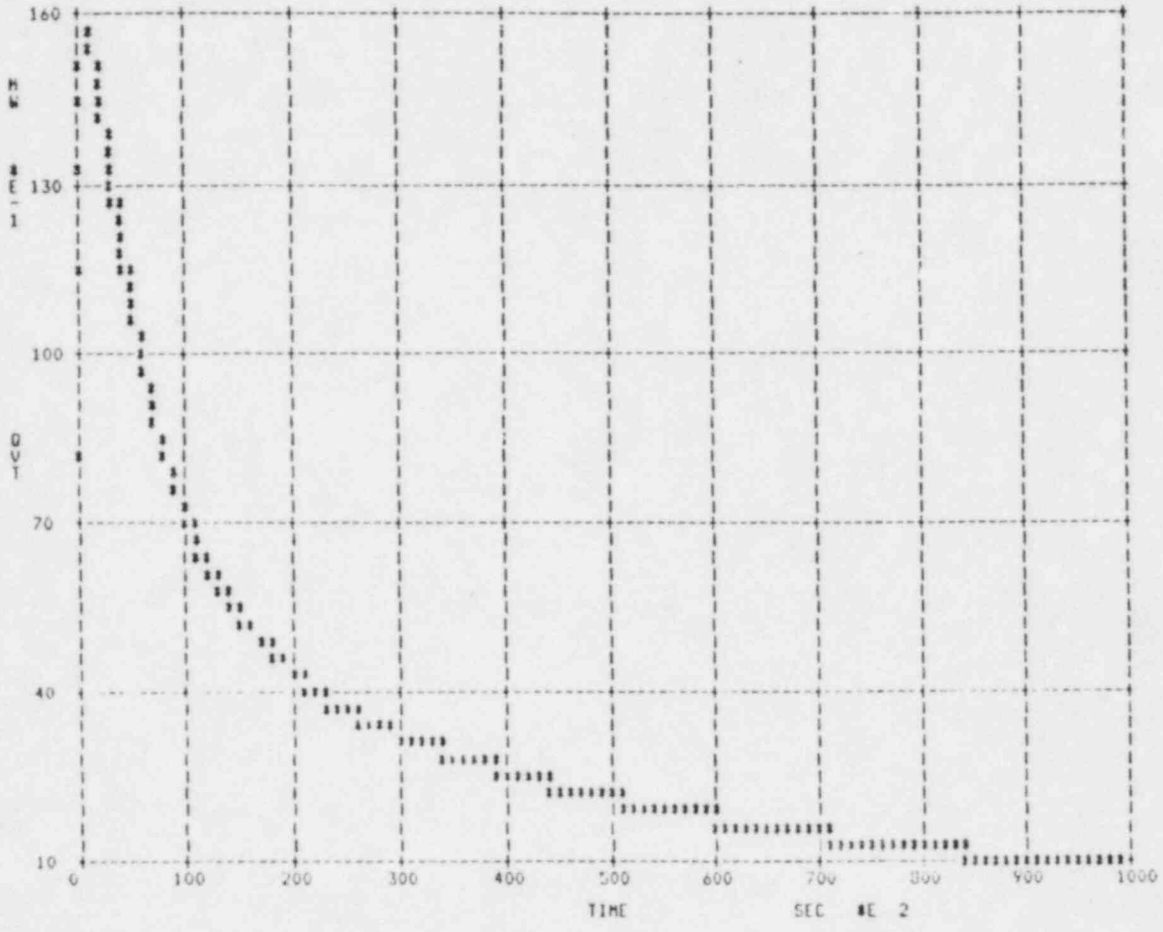

Fig. 4.11 Heat Removal Rate by Venting vs. Time for One Loop Natural Circulation.

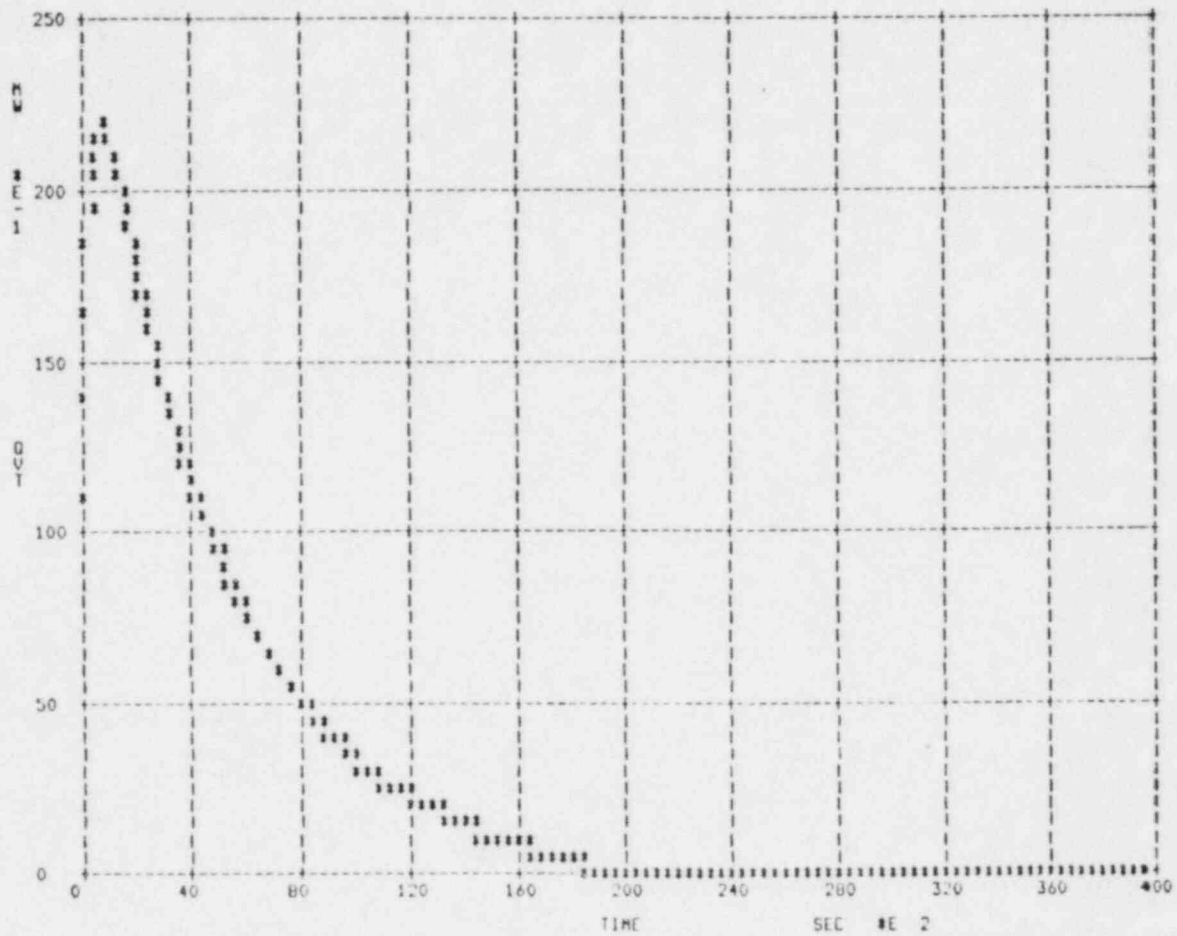

Fig. 4.12 Heat Removal Rate by Venting vs. Time for Two Loop Natural Circulation.

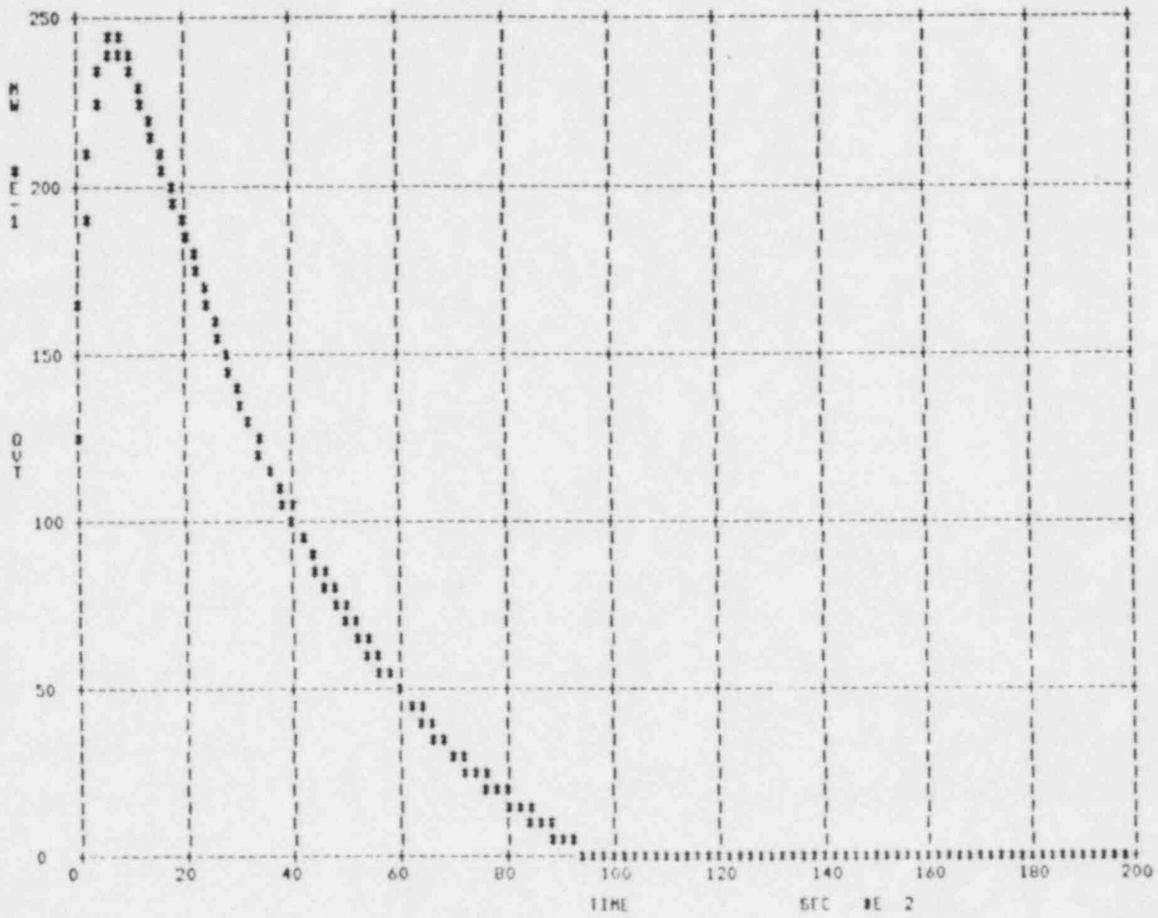

Fig. 4.13 Heat Removal Rate by Venting vs. Time for Three Loop Natural Circulation.

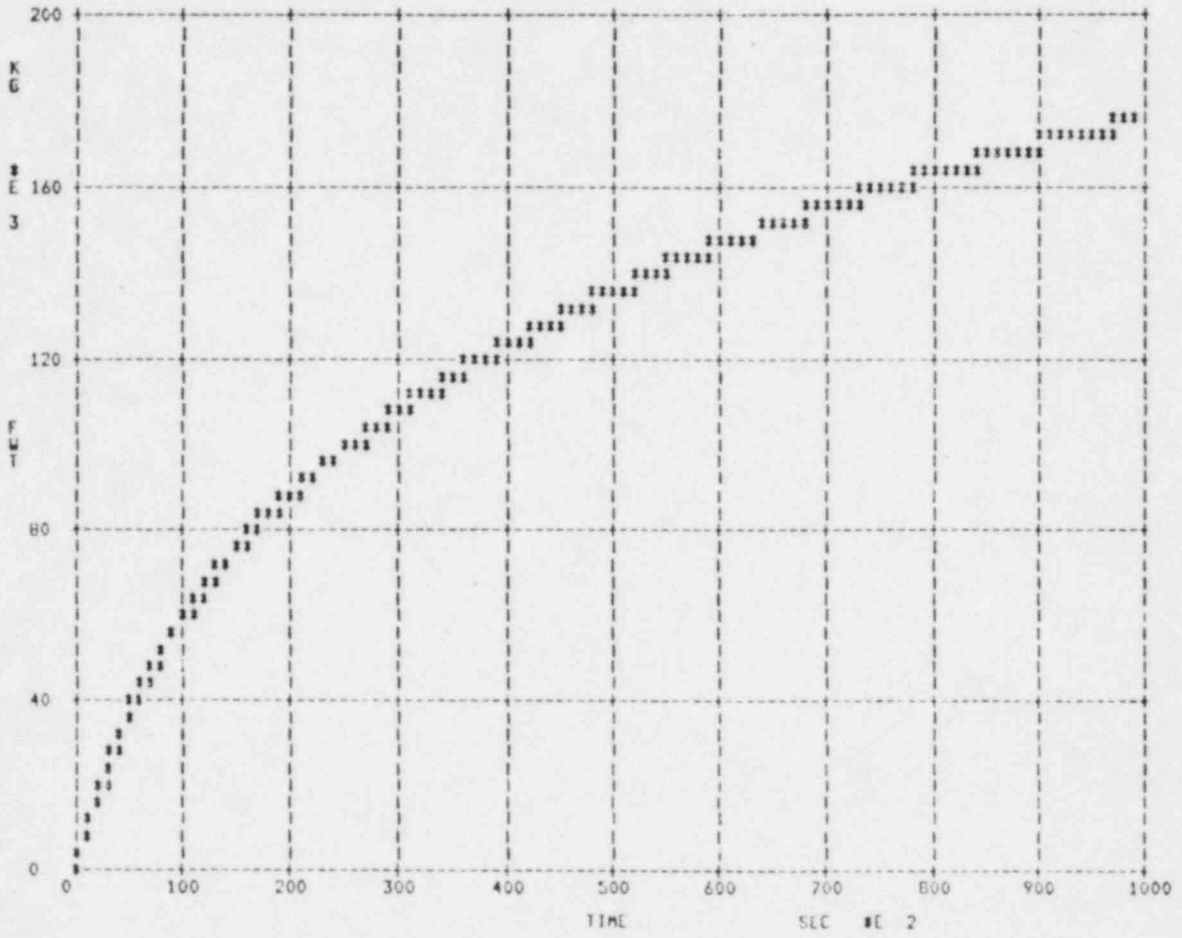

Fig. 4.14 Cumulative Mass of Steam Vented During a One Loop Natural Circulation Event.

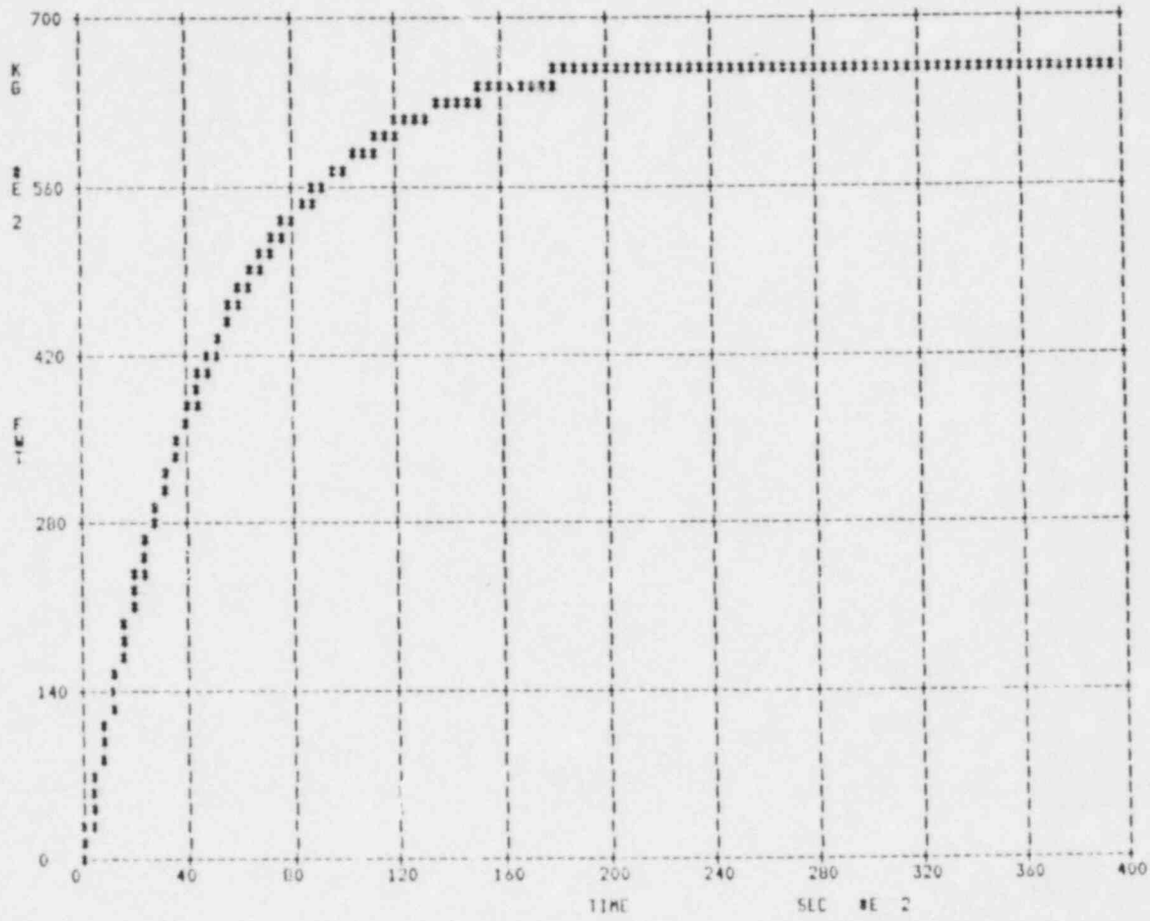

Fig. 4.15 Cumulative Mass of Steam Vented During a Two Loop Natural Circulation Event.

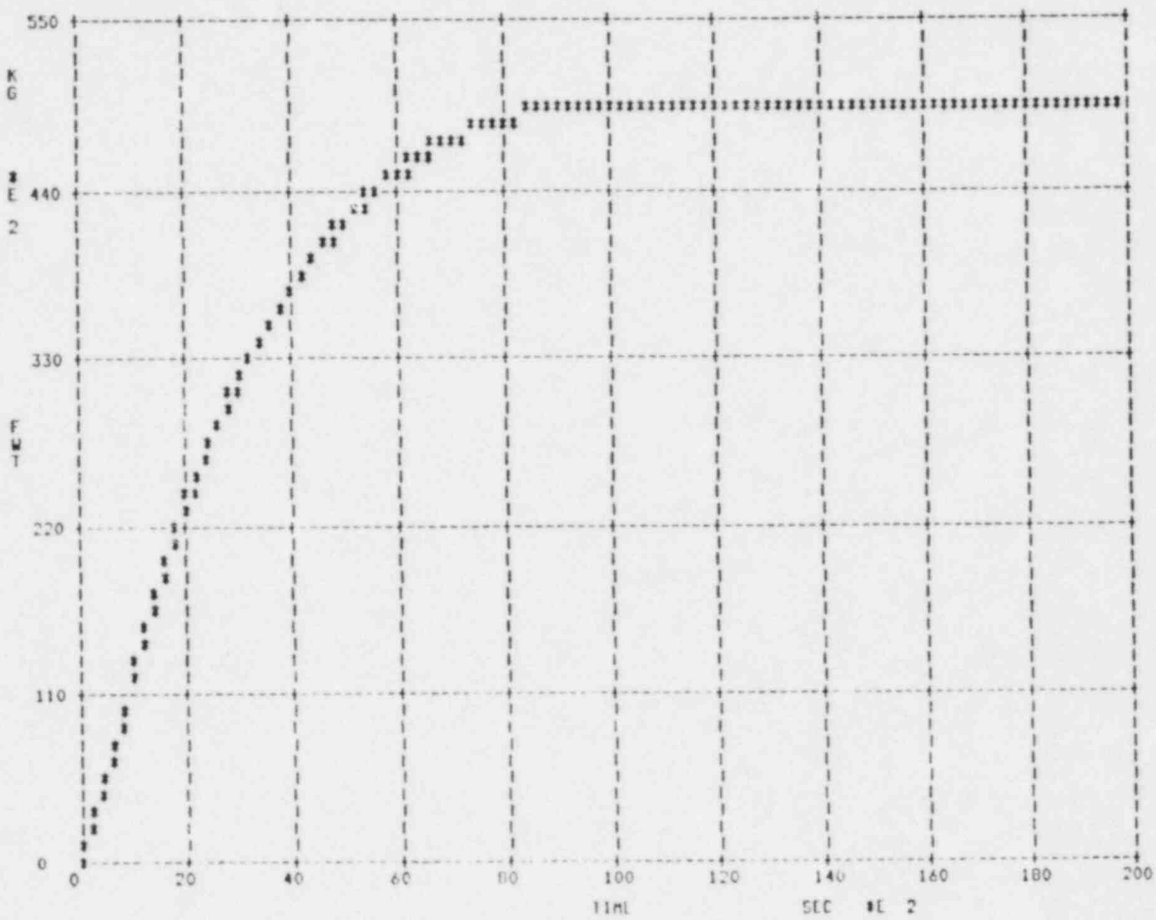

Fig. 4.16 Cumulative Mass of Steam Vented During a Three Loop Natural Circulation Event.

5.0 SUMMARY

The report has analyzed three areas of conservatism which is suitable for design purposes but is unneeded and undesirable for PRA purposes. Replacing the conservative quantities with best estimate one results in a number of benefits to the PRA study of a LOHS due to loss of all AC power and/or feedwater. Establishing sodium re-entry and dryout criteria results in at least a postponement of core damage for several hours. In less than 1/2 hour natural circulation heat removal under one loop operation is greater than decay power so the reactor could be cooled down with one loop if an adequate heat source is available.

The natural draft heat removal capability of the PACCs is substantial ($\sim$ 25-30% of the forced draft capacity). Using best estimate values in place of the conservative design ones results in predicting the cooldown of the system for about two hours of completely natural circulation operation without feedwater before the dry-out of the steam system. The study also shows that it would take several more hours (> 10 hours) to heat the system to a temperature at which core damage may occur. The availability of this additional time may prove to be very beneficial in a PRA study.

The difficulty in achieving cooldown without AC power and feedwater pumps is with the short term heat removal. The calculations predict that excessive steam would most likely be vented before the PACCs could assume the full load. However, some conservative assumptions were still used in obtaining these results and the removal of the conservatism should be investigated. One remaining area of conservatism is that of assuming the heat exchangers (IHX and evaporator) to be highly efficient, even as the water

inventory is decreasing. Analysis to obtain the best estimate values for heat exchanger efficiency is now being conducted.

6.0 REFERENCES

1. R. A. Bari, et al., "Accident Progression for a Loss-of-Heat-Sink with Scram in a Liquid-Metal Fast Breeder Reactor," Nuclear Technology, Vol. 44, August 1979.

2. K. R. Perkins, R. A. Bari, and W. T. Pratt, "In-Vessel Natural Circulation During a Hypothetical Loss-of-Heat-Sink Accident in the Fast Flux Test Facility," 79-WA/HT-66, Paper presented at the ASME Winter Annual Meeting, New York, New York, December 2-7, 1979.

3. H. Vossebrecker and A. Kellner, "Inherent Safety Characteristics of Loop-Type LMFBRs," Proc. Intl. Mtg. on Fast Reactor Safety Technology, Seattle, Washington, August 19-23, 1979.

4. T. C. Chawla and H. K. Fauske, "On the Incoherency in Subassembly Voiding in FTR and Its Possible Effect on the Loss-of-Flow Accident Sequence," Trans. Am. Nucl. Soc., Vol. 17, p. 285, 1973.

5. Kutateladze, "Elements of the Hydrodynamics of Gas-Liquid Systems," Fluid Mechanics - Soviet Res., Vol. 17, pp. 29-46, 1972.

6. Y. Katto, "A Generalized Correlation of Critical Heat Flux for the Forced Convection Boiling in Vertical Uniformly Heated Round Tubes," Intl. J. Heat Mass Transfer, Vol. 21, p. 1527, 1978.

7. M. Ishii and H. K. Fauske, "Boiling and Dryout Behavior in an LMFBR Subassembly Bundle Under Low Heat Flux and Low Flow Conditions," to be published, 1982.

8. CRBRP-ARD-0308, "Summary Report on the Current Assessment of the Natural Circulation Capability with the Heterogeneous Core," February 1982.

9. K. Chen, S.Wong, and D. Drendel, "Thermal Evaluation of the CRBR Protected Air Cooled Condenser," Draft Report, March 1, 1982.

10. F. Kreith, "Principles of Heat Transfer," International Textbook Company, 1958.